Acta Crystallographica Section D
Biological Crystallography
ISSN 0907-4449

The *CXXC* motif: crystal structure of an active-site variant of *Escherichia coli* thioredoxin

L. Wayne Schultz,[a] Peter T. Chivers[a]† and Ronald T. Raines[a,b]*

[a]Department of Biochemistry, University of Wisconsin–Madison, Madison, WI 53706, USA, and [b]Department of Chemistry, University of Wisconsin–Madison, Madison, WI 53706, USA

† Present address: Department of Biology, Massachusetts Institute of Technology, 77 Massachusetts Avenue, Cambridge, MA 02139, USA.

Correspondence e-mail: raines@biochem.wisc.edu

Received 26 April 1999
Accepted 24 June 1999

PDB Reference: CVWC thioredoxin, 1txx.

The 2.2 Å crystalline structure of an oxidized active-site variant of *Escherichia coli* thioredoxin (Trx) has been solved. Trx is a 12 kDa enzyme which catalyzes the oxidation of dithiols and the reduction and isomerization of disulfides in other proteins. Its active site contains the common structural motif C*XX*C. Protein-disulfide isomerase (PDI), a 57 kDa homolog of Trx, contains four Trx-like domains. The three-dimensional structure of PDI is unknown. PDI-deficient *Saccharomyces cerevisiae* are inviable. An active-site variant of Trx which complements PDI-deficient yeast has the active-site sequence Cys32-Val33-Trp34-Cys35 (CVWC). The reduction potential of oxidized CVWC Trx ($E^{\circ\prime}$ = −0.230 V) is altered significantly from that of the wild-type enzyme ($E^{\circ\prime}$ = −0.270 V). However, the structure of the oxidized CVWC enzyme is almost identical to that of wild-type Trx. The addition of valine and tryptophan in the active site is likely to increase the reduction potential, largely by decreasing the pK_a of the Cys32 thiol in the reduced enzyme. Unlike in wild-type Trx, significant protein–protein contacts occur in the crystal. Protein molecules related by a crystallographic twofold axis form a dimer in the crystal. The dimer forms as an extension of the twisted mixed β-sheet which composes the backbone of each Trx structure.

1. Introduction

Escherichia coli thioredoxin (Trx), a thiol–disulfide oxidoreductase, catalyzes the oxidation of dithiols and the reduction and isomerization of disulfides in other proteins (Gilbert, 1990). Trx is an 11.7 kDa enzyme with a polypeptide chain of 108 amino-acid residues. The structure of Trx, as described by X-ray crystallography (Holmgren *et al.*, 1975; Katti *et al.*, 1990) and NMR spectroscopy (Jeng *et al.*, 1994), is comprised of a five-stranded β-sheet containing parallel and antiparallel strands, surrounded by four α-helices. The active site is located at the N-terminus of an α-helix near the central portion of the β-sheet (residues 32–49). The active-site sequence, Cys-Gly-Pro-Cys (CGPC), is conserved among thioredoxins and is characteristic of the C*XX*C motif of thiol–disulfide oxidoreductases (Chivers *et al.*, 1998; Åslund & Beckwith, 1999).

Catalysis of disulfide-bond reduction or isomerization by Trx is initiated by deprotonation of the solvent-exposed N-terminal C*XX*C cysteine residue (Cys32) to form a thiolate. The reaction proceeds by nucleophilic attack of this thiolate on the substrate. To achieve maximal catalysis, the pK_a of the thiol must match the ambient pH (Gilbert, 1990). Generally, the pK_a of a cysteine thiol is near 9 and thus would be mostly protonated and unreactive at physiological pH. However, Cys32 has a microscopic pK_a near 7 (Chivers, Prehoda,

Volkman *et al.*, 1997). Nucleophilic attack by Cys32 results in the formation of an enzyme–substrate mixed disulfide. Cys35 is buried in the protein structure and has a pK_a near 11 (LeMaster, 1996; Chivers, Prehoda & Raines, 1997). General base catalysis by Asp26 enables Cys35 to attack Cys32, producing reduced substrate and oxidized Trx (Chivers & Raines, 1997; LeMaster *et al.*, 1997).

Another important feature of a C*XX*C motif is the reduction potential of its disulfide bond. Trx is the most reducing of the known thiol–disulfide oxidoreductases, having a reduction potential ($E^{\circ\prime}$) of −0.270 V (Moore *et al.*, 1964). Protein-disulfide isomerase (PDI), a homologous enzyme, has a reduction potential of $E^{\circ\prime}$ = −0.180 V (Lundström & Holmgren, 1993). PDI is a 55 kDa enzyme which consists of domains *a*, *b*, *b*′, *a*′ and *c* (Edman *et al.*, 1985; Pihlajaniemi *et al.*, 1987; Kemmink *et al.*, 1996). The *a* and *a*′ domains of PDI are structurally homologous to Trx and contain active sites of sequence Cys-Gly-His-Cys (CGHC) (Kemmink *et al.*, 1996). The *b* and *b*′ domains are homologous to Trx but do not contain C*XX*C active sites (Kemmink *et al.*, 1997). The *c* domain is not critical for enzyme function (Koivunen *et al.*, 1999). No three-dimensional structure has been reported for the intact enzyme. PDI is found in a variety of organisms, has been described as a chaperone and is the most efficient known catalyst of oxidative protein folding (Freedman, 1989; Noiva & Lennarz, 1992). In *Saccharomyces cerevisiae*, the essential function of PDI is to catalyze the isomerization of non-native disulfide bonds to native ones (Laboissière *et al.*, 1995).

The active-site sequences of PDI and Trx play a role in dictating the reduction potential, but are not the only determinants. Krause *et al.* (1991) introduced the PDI active-site sequence into Trx and determined the reduction potential ($E^{\circ\prime}$ = −0.235 V). The remaining difference in reduction potential between PDI and CGHC Trx ($\Delta E^{\circ\prime}$ = 0.055 V) represents nearly a 100-fold difference in the equilibrium stability of the C*XX*C disulfide bond. Chivers *et al.* (1996) selected for random mutations in the C*XX*C motif of Trx which would complement PDI-deficient yeast. Two such sequences, Cys-Val-Trp-Cys (CVWC; $E^{\circ\prime}$ = −0.230 V) and Cys-Gly-Trp-Cys (CGWC; $E^{\circ\prime}$ = −0.200 V), were found to do so. The ability to replace PDI arises from the increased thiolate concentration of the variant C*XX*C motifs.

Here, we report the crystalline structure of the oxidized CVWC variant of Trx refined to a resolution of 2.2 Å. The structure reveals that the substitutions cause few changes in the conformation of the protein, including the active-site disulfide bond. This finding is consistent with the increase in $E^{\circ\prime}$ largely arising from a decrease in thiol pK_a. In addition, we observe a crystallographic dimer of CVWC Trx mediated by crystal contacts.

2. Materials and methods

2.1. Protein crystallization

CVWC Trx was produced in *E. coli* and purified as described previously (Chivers, Prehoda, Volkman *et al.*, 1997).

Table 1
X-ray diffraction analysis statistics for CVWC thioredoxin.

Crystal data	
Space group	$P4_32_12$
Unit-cell dimensions (Å)	
a	42.53 (1)
b	42.53 (1)
c	105.24 (2)
Protein molecules per unit cell	8
Data-collection statistics	
Resolution (Å)	2.2
Number of measured reflections ($I/\sigma > 0.33$)	37820
Number of unique reflections	5979
Average redundancy	6.3
Average I/σ	20.1
Completeness (30–2.2 Å) (%)	98
Completeness, high-resolution shell† (%)	95
R_{sym}	0.083
R_{sym}, high-resolution shell†	0.173
Final refinement statistics	
Thioredoxin atoms	832
Solvent atoms	82
R factor (30–2.2 Å)	0.171
R.m.s. deviations from ideal geometry	
Bond distances (Å)	0.011
Bond angles (°)	2.27
Average *B* factors (Å^2)	
Main-chain atoms	25.7
Side-chain and solvent atoms	38.7
Cu^{2+}	48.5

† High-resolution shell, 2.3–2.2 Å.

Crystals of CVWC Trx were prepared by vapor diffusion using the hanging-drop method. Drops (6 µl) of 0.050 *M* sodium succinate buffer (pH 4.2) containing CVWC Trx (10 mg ml^{-1}), methyl ether PEG 2000 [10%(*w*/*v*)] and copper(II) acetate (1 m*M*) were suspended over wells (1.0 ml) of 0.10 *M* sodium succinate buffer (pH 4.2) containing methyl ether PEG 2000 [20%(*w*/*v*)] and copper(II) acetate (2 m*M*). A cat whisker was used to streak-seed the drops with microcrystals of CVWC Trx grown in a solution of high PEG concentration. The tetragonal crystals were grown at 293 K, appeared within one week and grew to final dimensions of 0.3 × 0.3 × 0.4 mm.

2.2. Data collection

Crystals of CVWC Trx belonged to space group $P4_32_12$, with unit-cell parameters *a* = 42.53, *c* = 105.24 Å and $\alpha = \beta = \gamma = 90^\circ$. X-ray data were collected with a Siemens HI-STAR detector mounted on a Rigaku rotating-anode generator operating at 50 kV and 90 mA with a 300 µm focal spot. The X-ray beam was collimated by double-focusing mirrors. The crystal-to-detector distance was 12.0 cm. Data were obtained in 512 × 512 pixel format, processed with the program *XDS* (Kabsch, 1988*a*,*b*) and scaled using the program *XSCALIBRE* (G. Wesenberg and I. Rayment, unpublished work). Frames of data (900 × 0.15° = 135°) were collected from a single crystal using a single φ scan. Reflections with I/σ < 0.33 were rejected. The crystal was cooled in a 277 K air stream, resulting in negligible crystal decay for the entire data collection. Full crystallographic details are listed in Table 1.

2.3. Molecular replacement

The structure was solved using the molecular-replacement routines in *AMoRe* (Navaza, 1994). The search model consisted of residues 1–31 and 36–108 of *E. coli* thioredoxin (PDB entry 2trx, molecule *A*) and was stripped of all solvent molecules. The rotation function was calculated using data from 15–3.5 Å, a 40 × 40 × 40 Å unit cell and a 15 Å sphere for self-vectors, and resulted in a single peak of 3.4 standard deviations above the next highest peak. The translation function was calculated using a 2 Å grid for the enantiomorphic space groups $P4_12_12$ and $P4_32_12$, resulting in *R* factors of 0.478 and 0.387, respectively. Ten cycles of rigid-body refinement were applied to the model in space group $P4_32_12$ and resulted in an *R* factor of 0.349.

2.4. Refinement

Prior to least-squares refinement, $2|F_o| - |F_c|$, $|F_o| - |F_c|$ and σ_A (Collaborative Computational Project, Number 4, 1994) difference maps were calculated using data in the resolution range 30–3.5 Å. The model was examined and was continuous in density for the entire chain. Three residues at the N-terminus were still not clearly defined in density and were removed. The starting model (residues 4–31 and 36–108) was subjected to ten cycles of least-squares refinement using *TNT* (Tronrud *et al.*, 1987) and data in the resolution range 30–3.0 Å, giving an initial *R* factor of 0.273. A difference Fourier map ($|F_o| - |F_c|$) clearly showed the position of residues 31–36. These residues were included in the model and refined to 2.5 Å. Manual adjustments to the model were performed in *TURBO-FRODO* (Cambillau *et al.*, 1997). After several cycles of manual adjustments and least-squares refinement, water molecules were added to the model. The peak-searching algorithm in *TNT* was used to place ordered water molecules. Water molecules were retained if they had at least 1σ of $2|Fo| - |F_c|$ density, 3σ of $|F_o| - |F_c|$ density and were within hydrogen-bonding distance of the protein or other water molecules. The density at the N-terminus became clearer and it was apparent that a Cu^{2+} ion, as also observed in the wild-type structure, was present. The Cu^{2+} ion was added to a 7σ peak in the $|F_o| - |F_c|$ density and refined. The N-terminal three residues were then fitted unambiguously to the density. The final model contains the complete protein (residues 1–108), 81 water molecules and one Cu^{2+} ion.

3. Results

The structure of CVWC Trx was solved by molecular replacement and refined to an *R* factor of 0.172 using data in the resolution range 30–2.2 Å (Fig. 1*a*). The r.m.s. deviations from target geometries are 0.011 Å for bond lengths and 2.27° for bond angles. Average *B* factors for the main chain and side chain are 25.7 and 38.7 Å^2, respectively. No *B*-factor restraints for bonded atoms were applied. The electron density is continuous for the main chain and most of the side chains. The conformation of residues 32–35 was unambiguous and clearly defined in both $2|F_o| - |F_c|$ density and annealed omit $|F_o| - |F_c|$ density (Fig. 1*b*). Strong density connecting Cys32 S^γ to Cys35 S^γ indicated the presence of a disulfide bond.

3.1. Comparison with wild-type thioredoxin

CVWC Trx has an overall structure almost identical to that of the wild-type enzyme. The main-chain atoms of CVWC Trx have an average r.m.s. deviation of 0.52 Å from those of wild-type thioredoxin molecule *A* (PDB entry 2trx). The greatest deviations occur in residues 1–3, with the main chain deviating up to 1 Å. When residues 1–3 were excluded, the r.m.s. deviation between CVWC Trx and the wild-type enzyme was 0.50 Å. The main chain also deviates by up to 1 Å at residues 10 and 20, which are found in surface loops of the protein. The

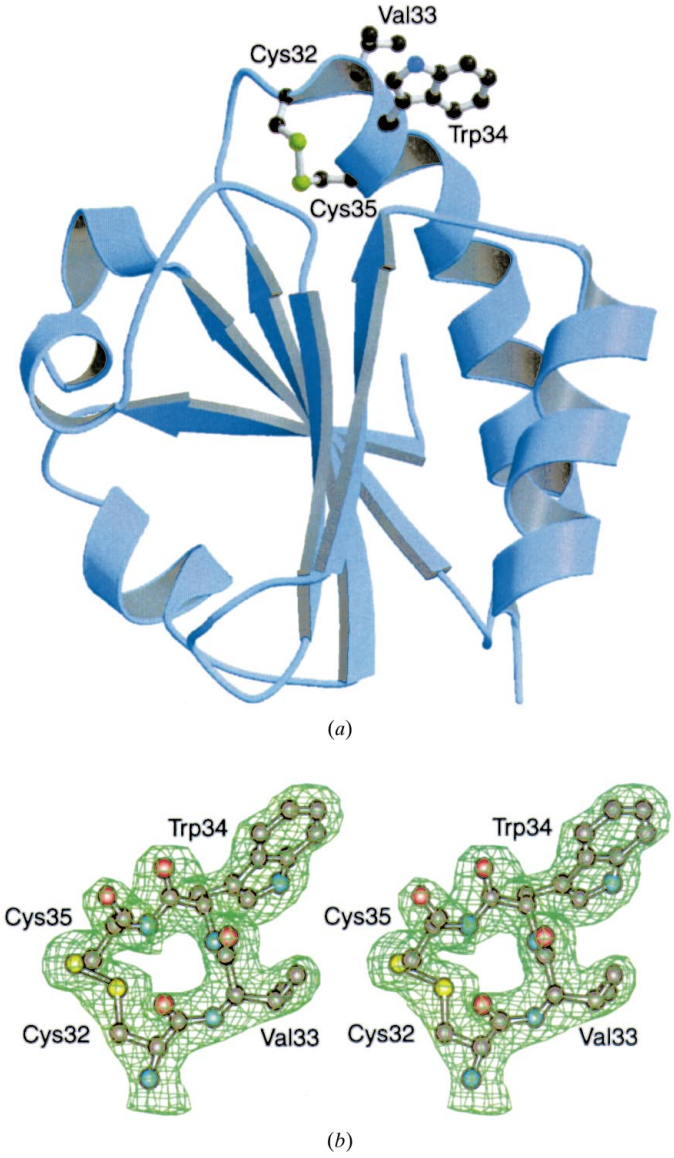

Figure 1
(*a*) Ribbon diagram of the CVWC variant of *E. coli* thioredoxin. The side chains of the C*XX*C motif are indicated. This figure was created with the program *MOLSCRIPT* v1.2 (Kraulis, 1991). (*b*) Active-site region of CVWC Trx. Electron density ($2|F_o| - |F_c|$) is contoured at 1.0σ. The views in (*a*) and (*b*) are from opposite sides of the molecule.

C-terminus has a slightly different conformation to that in wild-type Trx. The *B* factors for the two proteins are similar along the main chain.

3.2. Active-site structure

The substitutions at residues 33 and 34 in CVWC Trx do not create any significant changes in the structure. There is a significant rotation of the side chain of Trp31 owing to a crystal contact. The χ_1 and χ_2 angles are 40 and 86°, respectively, for wild-type Trx, and −56 and 107°, respectively, for the CVWC enzyme. The main-chain O atom of Trp31 forms a hydrogen bond of length 2.9 Å with the main-chain N atom of a symmetry-related Asp21. The main chain of residues 33 and 34 virtually overlaps with that of the wild-type enzyme. The side chains are in van der Waals contact with symmetry-related mates in the crystal. $N^{\varepsilon 1}$ of Trp34 makes the only hydrogen bond to a water molecule at a distance of 3.1 Å. The dihedral angles for residues 32–35 are typical of those found in an α-helix.

The disulfide bridge has angles similar to those found in wild-type Trx. The χ_1 and χ_2 angles of the side chains are 168 and −135°, respectively, for Cys32, and −67 and 86°, respectively, for Cys35. The torsion angle about $C^{\beta}-S^{\gamma}-S^{\gamma}-C^{\beta}$ is 67°. The $S^{\gamma}-S^{\gamma}$ bond length is 2.08 Å.

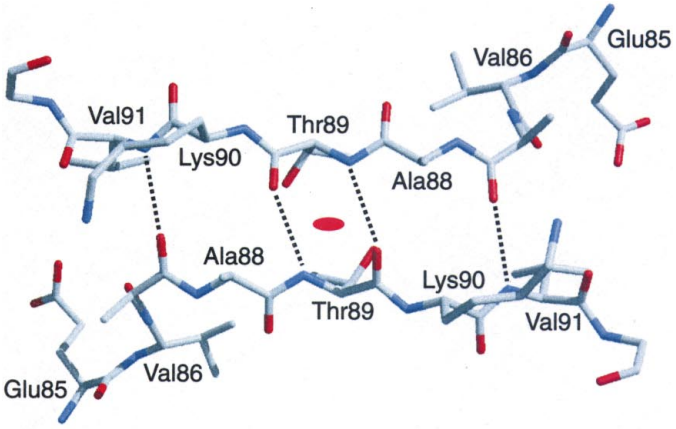

(*a*)

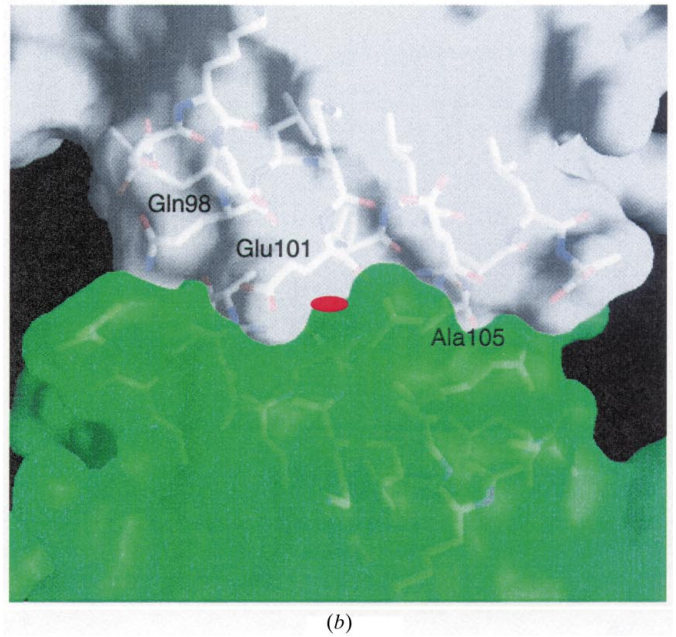

(*b*)

Figure 2
(*a*) β-Strand interaction at the crystal dimer interface of the CVWC variant of *E. coli* thioredoxin. Hydrogen bonds are shown as black dotted lines. (*b*) Molecular surfaces of C-terminal α-helices interacting at the dimer interface. The red ellipse indicates the location of the crystallographic twofold extending out from the plane. This figure was created with *GRASP* (Nicholls *et al.*, 1991).

3.3. Crystallographic dimer interface

Extensive contacts are made between the protein and a symmetry partner. The two molecules are related by a crystallographic twofold and the symmetry operator $(y, x, -z)$. The most extensive crystal contacts occur in residues 85–91 and in the C-terminal α-helix. Residues 85–91 form a β-strand at the edge of the β-sheet and form an antiparallel β-strand interaction with residues 91–85 of a symmetry mate (Fig. 2*a*). Residues 98–106 are in contact with the symmetry-related residues 106–98. The two helices fit together in a 'knobs-and-holes' fashion, with the side chains of residues 98 and 101 reaching over the side chain of residue 105 (Fig. 2*b*). Phe104 and its symmetry mate are buried at the interface but form an unfavorable edge-to-edge interaction at a distance of 3.61 Å. The interface buries 706 $Å^2$ of surface area.

3.4. Cu^{2+} binding

CVWC Trx, like the wild-type enzyme, requires copper(II) acetate for crystallization. This requirement exists even though the two enzymes crystallize in different space groups. The Cu atom in CVWC Trx is coordinated at the N-terminus by the main-chain N atoms of Ser1 and Asp2 and three water molecules in square-pyramidal geometry. In contrast, the wild-type coordination is a distorted octahedron and uses the side chains of Asp2 and a symmetry-related Asp10.

4. Discussion

4.1. Crystal packing and dimerization

CVWC Trx and wild-type Trx crystallized under similar conditions, yet produced different space groups. (Attempts to crystallize CVWC Trx under wild-type conditions failed.) Atomic coordinates of two other crystalline Trx variants have been determined [PDB entries 2tir (Nikkola *et al.*, 1993) and 1tho (M. Nikkola, K. Langsetmo, J. A. Fuchs & H. Eklund, unpublished results)]. Each Trx, including wild-type Trx and CVWC Trx, crystallized in a different space group. In the 2tir and 1tho structures, amino-acid substitutions introduce new hydrogen-bonding groups which make significant crystal contacts. The wild-type crystal form cannot accommodate Val33 and Trp34 of CVWC Trx because of steric and electrostatic conflicts. There are several intermolecular hydrogen bonds found in the CVWC structure which are not present in wild-type Trx and which result from crystal packing. However, only one specific hydrogen bond occurs near residues 33 and

34. The side chain of Trp31 rotates 98° around χ_1 and 170° around χ_2 with reference to wild-type Trx. This conformational change avoids a steric conflict with a symmetry-related residue. In addition, the main-chain O atom of Trp31 forms a hydrogen bond with the main-chain N atom of a symmetry-related Asp21. The main-chain O atom of Trp31 is available for hydrogen bonding in the wild-type structure; therefore, the structural change in Trp31 is not responsible for the change in space group, but is a result of the crystal packing.

The energetic cost of solvating a tryptophan side chain [$\Delta G_{\rm obs}$ = 3.07 kcal mol^{-1} (1 kcal mol^{-1} = 4.184 kJ mol^{-1})] or a valine side chain ($\Delta G_{\rm obs}$ = 1.66 kcal mol^{-1}) is high (Eisenberg & McLachlan, 1986). Desolvation of these residues could contribute significantly to crystal-lattice stability. In CVWC Trx, Val33 and Trp34 lie in a hydrophobic pocket created by hydrocarbons in the side chains of Lys3, Ile5 and Ile23, and Gln50 and Thr54 $C^{\gamma2}$ of a symmetry-related molecule. This hydrophobic interaction could drive the formation of the space group.

Interestingly, the copper ion is coordinated by a symmetry-related Asp10 side chain in both the wild-type and 1tho structures, even though these enzymes crystallized in different space groups. CVWC Trx also brings a symmetry-related Asp10 within 6.1 Å of the copper ion, but it is not involved in coordination.

CVWC Trx forms a dimer-like structure in the crystal. The largest number of protein–protein crystal contacts involve residues 85–91 from the β-sheet (Fig. 2*a*) and 98–106 from the C-terminal α-helix (Fig. 2*b*). The monomers come together at a crystallographic twofold axis with the β-sheets meeting edge-to-edge in antiparallel fashion. The resulting dimer forms a ten-stranded mixed parallel and antiparallel β-sheet. The C-terminal α-helix forms a 'knobs-and-holes' interaction with the C-terminal helix from a symmetry mate. In a favorable interaction, Phe104 is buried at the interface. There are no water-mediated contacts at the interface. The surface area buried by the dimer exceeds 700 Å^2, which is well within the range observed for protein dimers (Jones & Thornton, 1995). Gel-filtration chromatography and polyacrylamide gel electrophoresis suggest that CVWC Trx may exist as both monomers and dimers in solution (P. T. Chivers and R. T. Raines, unpublished results). In contrast, analytical ultracentrifugation of the CVWC enzyme revealed no significant dimer formation in solution at concentrations up to 30 µ*M* (data not shown). However, this concentration is significantly lower than that of the crystallization solution (1 m*M*).

E. coli Trx has never been shown to dimerize. Human Trx does dimerize in a crystalline state (Weichsel *et al.*, 1996), but this dimer differs significantly from that of CVWC Trx and is not present in solution (Gronenborn *et al.*, 1999). PDI contains four Trx domains, but there is little structural information available to describe the interaction of these domains. Recently, the structure of a protein-disulfide oxidoreductase from *Pyrococcus furiosus* (PDI_{Pf}) was reported (Ren *et al.*, 1998). This protein is a covalent dimer of two slightly different Trx-like domains. Like CVWC Trx, the domains come together to form a continuous β-sheet capped by two interlocked α-helices. However, the interface occurs at the opposite edge of the β-sheet to that of CVWC Trx. The dimers of CVWC Trx and PDI_{Pf} are topologically similar and either may represent a model for the interaction of the Trx-like domains of PDI.

4.2. Active site

The active site of Trx is found at the beginning of a long α-helix which protrudes from the enzyme (Fig. 1*a*). Located on the surface of the enzyme, Cys32 is poised to interact with a wide variety of substrates. Introduction of tryptophan and valine at positions 33 and 34 in Trx has no significant effect on the overall conformation of the oxidized active site. In CVWC Trx, the conformation of the Cys32–Cys35 disulfide bond and the position of Asp26 are almost identical to those in the wild-type enzyme (Fig. 1*b*). Yet, the CVWC variant has a higher reduction potential ($E^{\circ\prime}$ = −0.230 V) than wild-type Trx ($E^{\circ\prime}$ = −0.270 V), with $\Delta E^{\circ\prime} = E^{\circ\prime}_{\rm variant} - E^{\circ\prime}_{\rm wild\text{-}type}$ = 0.040 V (Chivers *et al.*, 1996).

Reduction potential is a measure of the relative stability of the dithiol and disulfide forms. An increase in reduction potential is an expression of the increased stability of the dithiol form relative to the disulfide form. This increase can arise from two factors: (i) a decrease in the pK_a of one or both thiols or (ii) an increase in the intrinsic reduction potential (ΔE°) of the disulfide bond (Chivers, Prehoda & Raines, 1997). In wild-type Trx and all known variants, Cys35 titrates at a pH >> 7 (Chivers, Prehoda, Volkman *et al.*, 1997). Hence, a change in the pK_a of the Cys35 thiol cannot contribute significantly to changes in $E^{\circ\prime}$ of CVWC Trx. In contrast, the value of $E^{\circ\prime}$ does depend on the pK_a of the Cys32 thiol, which titrates at pH ≤ 7. At 298 K, $\Delta E^{\circ\prime} = E^{\circ\prime}_{\rm variant} - E^{\circ\prime}_{\rm wild-type}$ is related to the pK_a of the Cys32 thiol by

$$\Delta E^{\circ\prime} \cong 0.03 \log\left(\frac{1 + 10^{\rm pH - pK_a^{variant}}}{1 + 10^{\rm pH - pK_a^{wild\ type}}}\right), \qquad (1)$$

which is derived from equation 5 in Chivers, Prehoda & Raines (1997). Given that $pK_a^{\rm wild\ type}$ = 7.50 and $pK_a^{\rm variant}$ = 6.16 (Chivers, Prehoda, Volkman *et al.*, 1997), then from (1) $\Delta E^{\circ\prime}$ = 0.023 V at pH 7.0. Thus, a change in the pK_a of the Cys32 thiol is responsible for most of the observed $\Delta E^{\circ\prime}$ of 0.040 V.

What is the structural basis for the change in the pK_a of the Cys32 thiol? Here, pK_a is a measure of the relative stabilities of the thiol and thiolate forms. In CVWC Trx, the pK_a of Cys32 is lower than that in wild-type Trx (Chivers *et al.*, 1996). Cys32 resides at the N-terminus of an α-helix (Fig. 1*a*). The thiolate form of Cys32 can be stabilized by the α-helix dipole (Forman-Kay *et al.*, 1991; Kortemme *et al.*, 1996). Introduction of the hydrophobic residues valine and tryptophan near the N-terminus may enhance this favorable Coulombic interaction. Indeed, calculations with the program *SYBIL* (version 6.5; Tripos, St Louis, MO, USA) indicate that the dipole moment of the α-helix formed by residues 32–49 increases by 17% in the CVWC variant (data not shown). In the more hydrophobic active site of the variant, the Cys32 thiolate

would be less shielded from the α-helix dipole by water and solute ions.

The decrease in the pK_a of the Cys32 thiol does not explain all of the increase in the reduction potential of the Cys32–Cys35 disulfide bond in CVWC Trx. The substitution in the C*XX*C motif must change the intrinsic reduction potential by $\Delta E^\circ \cong 0.017$ V. Replacing Pro33 could do so by increasing the conformational entropy of the dithiol form and thereby increasing the entropic cost of forming a disulfide bond. In addition, alterations in solvent structure within the active site could affect the value of ΔE°, as has been observed in pseudoazurin (Libeu *et al.*, 1997).

5. Conclusions

The C*XX*C motif is used by enzymes to catalyze the oxidation of dithiols and the reduction and isomerization of disulfide bonds. The activity of the C*XX*C motif relies upon a careful balance between reduction potential (dithiol–disulfide equilibrium) and pK_a (protonation state). The sequence of residues in the C*XX*C motif is a major contributor to setting the values of these parameters. CVWC Trx has an increased reduction potential and a decreased pK_a compared with those of wild-type Trx. Thus, addition of valine and tryptophan residues in the active site alters the catalytic properties of the enzyme without significantly altering the structure, at least of the oxidized enzyme.

This work was supported by grant BES-9604563 (NSF). LWS was supported by postdoctoral fellowship CA69750 (NIH). PTC was supported by a WARF Predoctoral Fellowship and a Steenbock Predoctoral Fellowship. We are grateful to Professor I. Rayment, Professor H. M. Holden and the members of their research groups for many helpful conversations and for the use of their X-ray data-collection and computational facilities, which are supported by grant BIR-9317398 (NSF).

References

Åslund, F. & Beckwith, J. (1999). *J. Bacteriol.* **181**, 1375–1379.
Cambillau, C., Roussel, A., Inisan, A. G. & Knoops-Mouthay, K. (1997). *TURBO-FRODO. Version* OpenGL.1. CNRS/Université Aix-Marseille II, Marseille, France.
Chivers, P. T., Laboissière, M. C. A. & Raines, R. T. (1996). *EMBO J.* **16**, 2659–2667.
Chivers, P. T., Laboissière, M. C. A. & Raines, R. T. (1998). *Prolyl Hydroxylase, Protein Disulfide Isomerase and Other Structurally Related Proteins*, edited by N. A. Guzman, pp. 487–505. New York: Marcel Dekker.
Chivers, P. T., Prehoda, K. E. & Raines, R. T. (1997). *Biochemistry*, **36**, 4061–4066.
Chivers, P. T., Prehoda, K. E., Volkman, B., Kim, B.-M., Markley, J. L. & Raines, R. T. (1997). *Biochemistry*, **36**, 14985–14991.
Chivers, P. T. & Raines, R. T. (1997). *Biochemistry*, **36**, 15810–15816.
Collaborative Computational Project, Number 4 (1994). *Acta Cryst.* D**50**, 760–763.
Edman, J. C., Ellis, L., Blacher, R. W., Roth, R. A. & Rutter, W. J. (1985). *Nature (London)*, **317**, 267–270.
Eisenberg, D. & McLachlan, A. D. (1986). *Nature (London)*, **319**, 199–203.
Forman-Kay, J. D., Clore, G. M., Wingfield, P. T. & Gronenborn, A. M. (1991). *Biochemistry*, **30**, 2685–2698.
Freedman, R. B. (1989). *Cell*, **57**, 1069–1072.
Gilbert, H. F. (1990). *Adv. Enzymol.* **63**, 69–172.
Gronenborn, A. M., Clore, G. M., Louis, J. M. & Wingfield, P. T. (1999). *Protein Sci.* **8**, 426–429.
Holmgren, A., Soderberg, B.-O., Eklund, H. & Branden, C.-I. (1975). *Proc. Natl Acad. Sci. USA*, **72**, 2305–2309.
Jeng, M.-F., Campbell, A. P., Begley, T., Holmgren, A., Case, D. A., Wright, P. E. & Dyson, H. J. (1994). *Structure*, **2**, 853–868.
Jones, S. & Thornton, J. M. (1995). *Prog. Biophys. Mol. Biol.* **63**, 31–65.
Kabsch, W. (1988*a*). *J. Appl. Cryst.* **21**, 916–924.
Kabsch, W. (1988*b*). *J. Appl. Cryst.* **21**, 67–71.
Katti, S. K., LeMaster, D. M. & Eklund, H. (1990). *J. Mol. Biol.* **212**, 167–184.
Kemmink, J., Darby, N. J., Dijkstra, K., Nilges, M. & Creighton, T. E. (1996). *Biochemistry*, **35**, 7684–7691.
Kemmink, J., Darby, N. J., Dijkstra, K., Nilges, M. & Creighton, T. E. (1997). *Curr. Biol.* **7**, 239–245.
Koivunen, P., Pirneskoski, A., Karvonen, P., Ljung, J., Helaakoski, T., Notbohm, H. & Kivirikko, K. I. (1999). *EMBO J.* **18**, 65–74.
Kortemme, T., Darby, N. J. & Creighton, T. E. (1996). *Biochemistry*, **35**, 14503–14511.
Kraulis, P. (1991). *J. Appl. Cryst.* **24**, 946–950.
Krause, G., Lundström, J., Barea, J. L., Pueyo de la Cuesta, C. & Holmgren, A. (1991). *J. Biol. Chem.* **266**, 9494–9500.
Laboissière, M. C. A., Sturley, S. L. & Raines, R. T. (1995). *J. Biol. Chem.* **270**, 28006–28009.
LeMaster, D. M. (1996). *Biochemistry*, **35**, 14876–14881.
LeMaster, D. M., Springer, P. A. & Unkefer, C. J. (1997). *J. Biol. Chem.* **272**, 29998–30001.
Libeu, C. A. P., Kukimoto, M., Nishiyama, M., Horinouchi, S. & Adman, E. T. (1997). *Biochemistry*, **36**, 13160–13179.
Lundström, J. & Holmgren, A. (1993). *Biochemistry*, **32**, 6649–6655.
Moore, E. C., Reichard, P. & Thelander, L. (1964). *J. Biol. Chem.* **239**, 3445–3452.
Navaza, J. (1994). *Acta Cryst.* A**50**, 157–163.
Nicholls, A., Sharp, K. A. & Honig, B. (1991). *Proteins Struct. Funct. Genet.* **11**, 281–296.
Nikkola, M., Gleason, F. K., Fuchs, J. A. & Eklund, H. (1993). *Biochemistry*, **32**, 5093–5098.
Noiva, R. & Lennarz, W. J. (1992). *J. Biol. Chem.* **267**, 3553–3556.
Pihlajaniemi, T., Helaakoski, T., Tasanen, K., Myllylä, R., Huhtala, M.-L., Koivu, J. & Kivirikko, K. I. (1987). *EMBO J.* **6**, 643–649.
Ren, B., Tibbelin, G., de Pascale, D., Rossi, M., Bartolucci, S. & Ladenstein, R. (1998). *Nature Struct. Biol.* **5**, 602–611.
Tronrud, D. E., Ten Eyck, L. F. & Matthews, B. W. (1987). *Acta Cryst.* A**43**, 489–501.
Weichsel, A., Gasdaska, J. R., Powis, G. & Montford, W. R. (1996). *Structure*, **4**, 735–751.